

10. Ramachandran GN, Lakshminarayanan AV. Three-dimensional reconstruction from radiographs and electron micrographs: application of convolutions instead of Fourier transforms. *Proc Natl Acad Sci* 1971;68:2236-2240.
11. Spinks TJ, Jones T, Gilardi MC, Heather JD. Physical performance of the latest generation of commercial positron scanner. *IEEE Trans Nucl Sci* 1988;35:721-725.
12. Robb RA, Hanson DP. A software system for interactive and quantitative visualization of multidimensional biomedical images. *Aust Phys Eng Sci Med* 1991;14:9-30.
13. Hoffman EJ, Huang SC, Plummer D, Phelps ME. Quantitation in positron emission tomography: 6. Effect of non-uniform resolution. *J Comput Assist Tomogr* 1982;6:987-999.
14. Woods RP, Cherry SR, Mazziotta JC. Rapid automated algorithm for alignment and reslicing PET images. *J Comput Assist Tomogr* 1992;16:620-633.
15. Shepp LA, Vardi Y. Maximum likelihood reconstruction for emission tomography. *IEEE Trans Med Imag* 1982;MI-1:113-122.
16. Lange K, Carson RE. EM reconstruction algorithms for emission and transmission tomography. *J Comput Assist Tomogr* 1984;8:306-316.
17. Silverman BW, Jones MC, Wilson JD, Nychka DW. A smoothed EM approach to indirect estimation problems, with particular reference to stereology and emission tomography. *J R Statist Soc* 1990;52:271-324.
18. Miller MP. Assessment of scatter radiation in PET scanning of the liver with labelled anticancer drugs [MSc thesis]. Surrey, United Kingdom: University of Surrey; 1995.
19. Hudson HM, Larkin RS. Accelerated image reconstruction using ordered subsets of projection data. *IEEE Trans Med Imag* 1994;13:601-609.
20. Wilson DW, Tsui BMW. Noise properties of filtered-backprojection and ML-EM reconstructed emission tomographic images. *IEEE Trans Nucl Sci* 1993;NS-40:1198-1203.
21. Meikle SR, Hutton BF, Bailey DL, Hooper PK, Fulham MJ. Accelerated EM reconstruction in total body PET: potential for improving tumour detectability. *Phys Med Biol* 1994;39:1689-1704.
22. Hoffman EJ, Huang SC, Phelps ME. Quantitation in positron emission tomography. Effect of object size. *J Comput Assist Tomogr* 1979;3:229-308.

Locally Increased Uptake of Fluorine-18-Fluorodeoxyglucose After Intracavitary Administration of Iodine-131-Labeled Antibody for Primary Brain Tumors

Christopher J.C. Marriott, Wade Thorstad, Gamal Akabani, Mark T. Brown, Roger E. McLendon, Michael W. Hanson and R. Edward Coleman

Department of Nuclear Medicine, London Health Sciences Centre, London, England; and Departments of Radiology and Pathology and Division of Neurology, Duke University Medical Center, Durham, North Carolina

After the intracavitary administration of ^{131}I -labeled monoclonal antibody for treatment of primary brain tumors after surgical resection, a persistent rim of ^{18}F -fluorodeoxyglucose (FDG) accumulation surrounding the cavity can be observed on PET. This rim, although it accumulates more FDG than adjacent normal brain tissue, is not necessarily associated with tumor. In our study, we examine the characteristics of the rim that indicate persistent tumor and tumor progression. **Methods:** Sequential PET studies obtained after treatment in 10 patients were reviewed and the results correlated with dosimetry and post-treatment histologic diagnoses. **Results:** The rim of FDG accumulation was seen on the first post-treatment scan obtained 1-3 mo after therapy and persisted unchanged over the 2-26 mo follow-up period. Pathologically, the nonmalignant rim was associated with marked increase of macrophage infiltrates. Nodularity of the rim was associated with tumor. **Conclusion:** Our study demonstrates that a rim of FDG accumulation is seen after intracavitary administration of ^{131}I -labeled monoclonal antibody therapy independent of the presence of malignant disease. Malignant recurrence is suggested by the development of new nodularity in the rim of FDG accumulation.

Key Words: PET; primary brain tumors; iodine-131-monoclonal antibody; fluorine-18-fluorodeoxyglucose

J Nucl Med 1998; 39:1376-1380

Survival of patients with certain brain tumors, particularly glioblastoma multiforme and anaplastic astrocytoma, has remained poor despite aggressive multimodal therapy of conventional surgery, antineoplastic chemotherapy and external beam radiation therapy (1). Conventional external beam radiotherapy is limited to a dose of approximately 60 Gy, using standard

fractionation, because of the effects on normal brain tissue (2,3). Various methods such as interstitial brachytherapy and stereotactic radiosurgery have been used to increase the radiation dose delivered locally to the tumor (4,5). An additional 12-15 Gy and 50 Gy can be delivered to the tumor with stereotactic radiosurgery and brachytherapy, respectively (6,7).

An alternate approach is to use a radiolabeled monoclonal antibody (MAb) reactive with tumor-associated antigen to target radiation delivery to the tumor site (8). The tumor absorbed dose can be increased by administering the radiolabeled MAb directly to tumor sites (i.e., intrathecally, into cystic tumor cavities or into postoperative cystic resection cavities) (9). Using intracavitary administration of ^{131}I -labeled MAb, doses of up to 1000 Gy can be delivered to cavity walls without hematologic toxicity.

Morphologic brain imaging using CT or MRI cannot always differentiate between recurrent or residual tumor and areas of necrosis after radiation therapy or chemotherapy of primary brain tumors (10). Low metabolic activity as determined by the absence of ^{18}F -fluorodeoxyglucose (FDG) uptake on PET in an area of contrast enhancement on CT or MRI indicates necrosis, whereas high metabolic activity suggests tumor. On FDG PET scans after intracavitary MAb treatment, however, we have noted metabolic activity greater than that found in adjacent normal brain tissue immediately surrounding the treatment cavity. We denote this region of uniform thickness along the cavity wall as a rim. Similarly, on MRI, a thin rim of enhancement surrounding the treatment cavity is noted. This metabolic activity often appears to be unrelated to tumor progression. In this context, the differentiation between this MAb treatment effect and recurrent or residual tumor becomes difficult. To evaluate the significance of the metabolic rim, with respect to its clinical and biologic implications, we retrospectively analyzed the patterns of metabolic activity

Received Jun. 9, 1997; revision accepted Nov. 21, 1997.

For correspondence or reprints contact: R. Edward Coleman, MD, Box 3949, Duke University Medical Center, Durham, NC 27710.

TABLE 1
Patient Characteristics at Initial Diagnosis

Patient	Age (yr)	Sex	Histologic tumor type	Previous external beam radiation (cGy)	Administered activity (MBq)	Administered monoclonal antibody (mg)
1*	37	M	Anaplastic oligodendroglioma	6,000	740	10
2*	13	F	Ependymoma	NA	2,960	9.9
3*†	64	M	Glioblastoma multiforme	6,120	4,440	20
4*‡	19	F	Glioblastoma multiforme	6,120	740	9.9
5*	30	M	Anaplastic astrocytoma	6,140	3,700	20
6*	54	M	Glioblastoma multiforme	4,600	2,220	9.7
7	44	M	Glioblastoma multiforme	0	560	10
8	29	M	Anaplastic astrocytoma	0	2,220	10
9	42	M	Glioblastoma multiforme	0	2,960	10
10	28	F	Astrocytoma	0	800	10

*These patients received prior radiation therapy.

†This patient had two biopsies.

‡This patient had two treatments and two biopsies. The second treatment was performed 26 mo after the first.

NA = not available.

surrounding the treatment cavity and correlated the results with either long-term survival or histopathology.

MATERIALS AND METHODS

Patients

Since 1988 more than 130 patients have received radiolabeled MAb therapy as part of Phase I/II trials of ¹³¹I-81C6, which is a radiolabeled murine IgG_{2b} MAb that reacts with an epitope of tenascin, an extracellular matrix antigen present in glioma cell lines and primary human gliomas. For our study, a subset of patients who received ¹³¹I-81C6 in surgically created cystic cavities that did not communicate with the cerebrospinal fluid space were studied. The tumors were demonstrated to be immunohistologically reactive with 81C6 before therapy. To be included in the protocol, patients could not have residual tumor extending more than 1 cm from the resection cavity, as determined on CT or MRI. Cohorts of three to six patients were treated with escalating dosages of ¹³¹I-labeled MAb. The starting dose was 740 MBq, with 740 MBq escalation in subsequent cohorts. As part of the protocol, patients underwent PET and MRI before and after treatment. Unless there was clear evidence of tumor progression, no additional radiotherapy was allowed in the first 3 mo after MAb treatment and no

additional antineoplastic chemotherapy could be administered for 6 wk. Patients could, however, have received either radiation or chemotherapy before MAb treatment.

Ten milligrams of ¹³¹I-labeled MAb were administered into the cystic cavity. For administered doses greater than 3700 MBq, 20 mg of MAb were used to decrease the radiation damage to the protein (11).

Among the patients treated with intracavitary MAb, eight had tissue samples of the cavity walls obtained after treatment. These samples were obtained either by stereotactic biopsy or resection of suspected tumor. Although stereotactic needle biopsy is limited with respect to volume sampling, it remains state of the art for diagnosing focal brain lesions. A longitudinal analysis of sequential PET studies of these eight patients was performed. Two additional patients who had a metabolic rim and long-term survival of more than 40 mo were included in the analysis. Patient characteristics are described in Table 1.

Patients received a bolus injection (5.3 MBq/kg, 0.144 mCi/kg) of FDG in a quiet, dimly lit room. After a 30-min uptake period, PET was performed using an Advance PET scanner [General Electric (GE) Medical Systems, Milwaukee, WI], except for Patients 8 and 10, whose sequential studies were

TABLE 2
Cavity Volume, Dosimetry and MRI Rim Enhancement

Patient	Cavity volume (cm ³)	Administered activity (MBq)	Estimated dose to the interface (cGy)	Rim thickness (cm)*
1	45	740	1,600	NA
2	59	2,960	5,000	0.3
3	15	4,440	27,900	0.3
4†	10	740	7,000	0.2
	10	4,440	41,900	0.3
5	3	3,700	133,400	NA
6	11	2,220	31,300	0.3
7‡	5	560	22,800	NA
8	18	2,220	11,700	0.3
9	10	2,960	28,700	0.4§
10	20	800	3,800	0.3

*Measured on first MR image obtained after treatment.

†This patient received two treatments.

‡CT was used for cyst volume calculations and follow-up.

§Rim thickness decreased slightly to 0.3 mm 8 mo after treatment.

NA = not available.

TABLE 3
Results of FDG PET Scans and Biopsies

Patient	Pretreatment PET findings*		First post-treatment PET (mo)	Findings*		Months of post-treatment stable PET	Months to biopsy†	PET findings immediately before biopsy*		Post-treatment histology
	Rim	Nodule		Rim	Nodule			Rim	Nodule	
1	0	0	1	2	0	5	1	2	0	Reactive, marked inflammatory cells
2	0	0	1	3	0	17		Unchanged	-17 mo	
3‡	0	0	2	2	0	10	3	2	0	Gliosis and necrosis
	0	0	2	2	0	10	10	2	0	Marked macrophage infiltrate
4§	0	2	2	0	2	22	26	0	3	High-grade glioma
			1	2	0	7	7	2	0	Extensive necrosis and 1-min focus of glioma
5	0	3	1	2	3	1	2	2	3, 3¶	GBM and therapeutic effect
6	2	0	1	2	0	3	6	1	4	GBM
7	3	0	1	3	0	4	13	0	0, no cyst	High-grade glioma
8	0	0	1	0	0	4	13	0	2	GBM and therapeutic effect
9	0	3	3	2	0	4	6	2	3, 3¶	Necrosis and extensive glioma
10	1	0	1	2	0	19		Unchanged	-19 mo	

*Activity is graded. None = 0; < white matter = 1; between white and gray matter = 2; equal to gray matter = 3; > gray matter = 4.

†Time from monoclonal antibody therapy to biopsy.

‡This patient had two biopsies.

§This patient had two treatments and two biopsies.

¶Two isolated regions of nodular metabolism noted.

GBM = glioblastoma multiforme.

performed using a GE PC 4096 PET scanner (12). Calculated attenuation correction was performed, and images were presented in sagittal, coronal and transaxial planes for interpretation.

Sequential PET studies, from before the MAb treatment to the time of stereotactic biopsy or resection, were interpreted without the anatomic imaging studies by two experienced nuclear medicine physicians. The final interpretation was obtained by consensus. The final study obtained before biopsy was interpreted initially without knowledge of previously completed studies and again in temporal sequence compared with previous studies. Because the interpretation of this PET study was the same in isolation or in comparison with previous studies, the parameters used to assess the cystic cavity were judged to be reasonably robust. Several parameters were used to characterize the pattern of metabolic activity as reflected by FDG uptake. A rim was present if a thin band of uniform thickness with FDG uptake greater than adjacent normal brain tissue was noted along the cavity walls. The FDG uptake in the rim was graded as 1, if less than that of normal white matter; 2, if between gray and white matter; 3, if equal to gray matter; and 4, if greater than gray matter. Nodular uptake was defined as an area of increased thickness or uptake in a uniform rim or a focal area of increased FDG accumulation.

On MRI, a thin persistent rim of enhancement was noted surrounding the treatment cavity in every patient included in this study. The thickness of this rim was measured on multiple MR scans obtained after treatment. In addition, cavity volume was estimated from pretreatment MRI images.

Dosimetry

By taking into account the biokinetics of the ¹³¹I-labeled MAb obtained from whole-body planar imaging in a subset of treatment patients and the pretreatment cavity volume, the dose delivered to the cavity wall and immediately surrounding tissue was estimated assuming a spherical cavity (13).

RESULTS

Of the 10 patients included in this study (Table 1), 6 had a diagnosis of glioblastoma multiforme, 2 had anaplastic astro-

cytoma, 1 had ependymoma and 1 had astrocytoma. Two patients underwent biopsy twice after treatment, and one patient received two treatments. Two to 14 post-treatment PET studies were obtained for each patient. The initial post-treatment scan was obtained 1–3 mo after treatment. The administered ¹³¹I activity ranged from 740 to 4400 MBq (20–120 mCi). Cavity

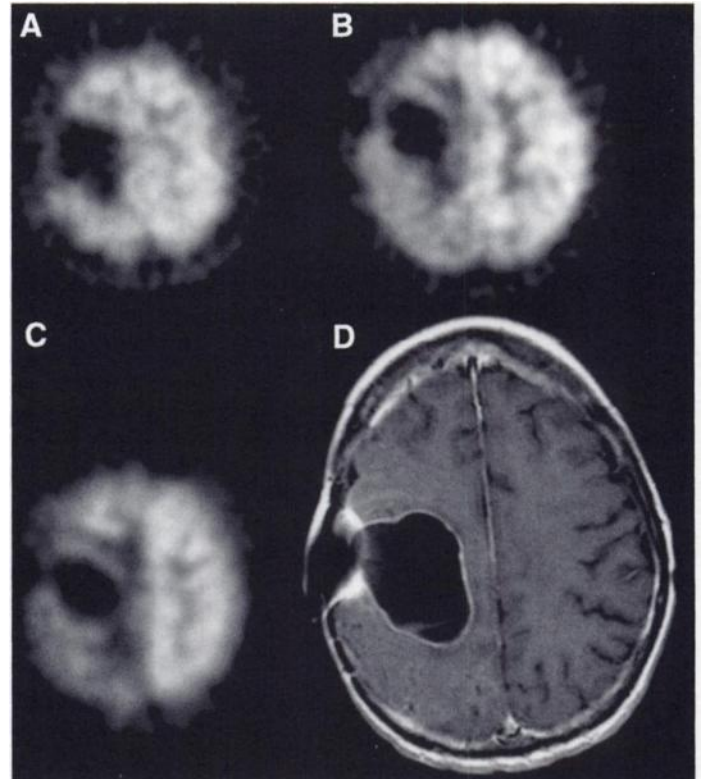


FIGURE 1. Example of the time course of the metabolic rim on FDG PET scan (Patient 2). (A) Pretreatment study demonstrates no rim. (B) First post-treatment scan at 1 mo reveals a metabolic rim. (C) Scan obtained at 18 mo shows a metabolic rim that is unchanged from the scan at 1 mo. (D) Uniform rim of enhancement is noted on MRI 1 mo after therapy.

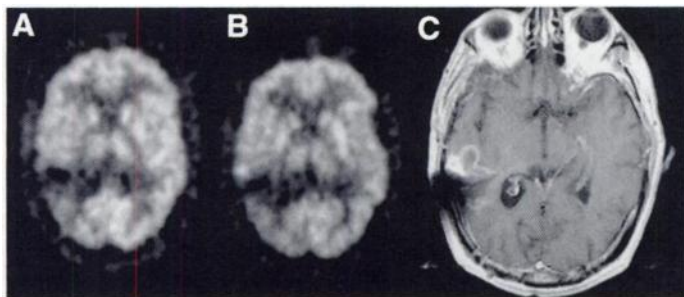


FIGURE 2. Example of new nodular metabolism on FDG PET scan consistent with recurrent disease (Patient 3). (A) Post-treatment scan at 3 mo demonstrates a cystic resection cavity. (B) Scan obtained 6 mo after treatment shows new nodular focus of FDG accumulation (Grade 4). (C) MR image obtained at 6 mo after treatment shows new contrast-enhancing lesion at site of abnormal FDG accumulation.

volume, the estimated radiation dose absorbed at the cavity-brain interface and measured thickness of the MRI-enhancing rim are given in Table 2.

The sequential PET imaging findings are presented in Table 3. All times are measured with respect to the MAb treatment date. The duration of the findings on the first post-treatment scan that was unchanged on subsequent PET studies is reported as number of months of stable PET. The four patients with benign changes, either by biopsy results (Patients 1 and 3) or long-term survival (Patients 2 and 10), had nonmodular hypermetabolic rims on post-treatment PET scans (Fig. 1). Seven biopsies revealed malignant histology, and five of the PET scans (Patients 4, 5, 6, 8 and 9) had an area of nodular FDG accumulation at the time of biopsy (Fig. 2).

Two patients (4,7) had malignant histology and no nodular abnormalities on the PET scan. Patient 7 had recurrence documented by biopsy. The recurrent tumor was in the region of the cortical gray matter that was not detected as different from normal gray matter on the PET scan. Patient 4 received two MAb treatments and had a focus of nodular hypermetabolism before resection that proved to be a recurrent glioma. The initial 740-MBq (20-mCi) treatment did not produce a visible rim of increased FDG uptake. The second 4400-MBq (120-mCi) treatment did, however, produce a metabolic rim. Results from

the second biopsy demonstrated a very small focus of low-grade tumor.

DISCUSSION

This study demonstrates that a metabolic rim of activity on FDG imaging can result from the intracavitary administration of ^{131}I -labeled MAb in patients who have had surgical resection of primary brain tumors. If a metabolic rim occurs, it is seen on the first post-treatment scan and persists with little change thereafter. Rozenal et al. (14) studied FDG accumulation by PET scanning in the first week after stereotactic radiotherapy. They delivered a dose of 105 Gy to the tumor and reported increased FDG accumulation occurring in the first week after treatment. Patient 4 in our study received two administered doses of 740 MBq and 4440 MBq. The higher dose produced a metabolic rim on the PET scan. In the small number of patients in this study, there is the suggestion that the development of a metabolic rim is dose dependent, with higher doses producing a rim of increased FDG accumulation.

In regions with no tumor progression, the thickness of the MRI contrast-enhancing rim remained constant after treatment. Its thickness was between 0.3 and 0.4 cm. A similar 0.6–0.8 cm enhancing rim has been reported to persist for at least 18 mo (the duration of post-treatment follow-up) after ^{125}I interstitial brachytherapy (15–17).

Because increased FDG uptake in a uniform rim does not accurately predict tumor recurrence, an additional criterion must be used. Recurrent tumor was found in nodular areas that demonstrated increased FDG accumulation. Patient 6 (Fig. 2) presented with a new focus of hypermetabolism, and biopsy results demonstrated recurrent glioblastoma multiforme.

Histologically, the metabolic rim is associated with an inflammatory infiltrate that appears to have a relatively increased number of macrophages and fibroblasts (Figs. 3 and 4). The number of inflammatory cells in biopsy samples of a metabolic rim is greater than that usually observed in brain tissue evaluated after trauma and infarction. Patient 4, who had no metabolic rim after the first treatment, did not have a markedly increased number of macrophages demonstrated on the first biopsy, which did document high-grade glioma. In the presence of a metabolic rim, however,

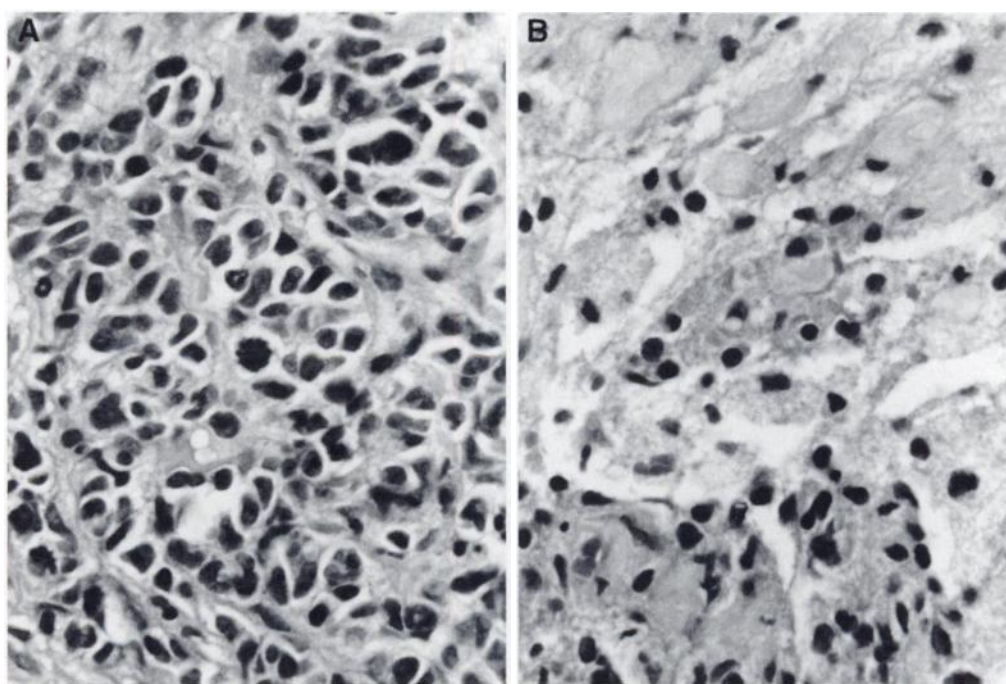


FIGURE 3. Histopathology (Patient 1). (A) Primary resection. Tissue sample from original resection reveals a neoplasm characterized by round eosinophilic cells with hyperchromatic, mitotically active nuclei of anaplastic oligodendroglioma (H&E, X680). (B) Secondary resection 1 mo after ^{131}I -81C6 monoclonal antibody treatment. Tissue sample from second resection reveals dense infiltrate of macrophages ("gitter" cells) characterized by foamy cytoplasm and round regular nuclei (H&E, X680).

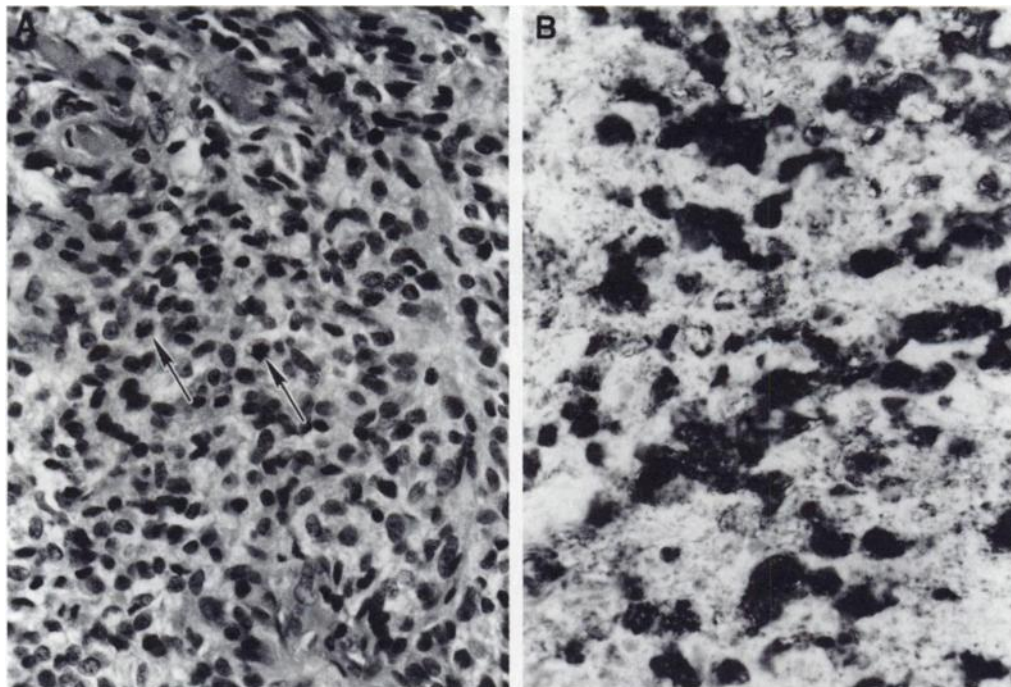


FIGURE 4. Histopathology (Patient 3). (A) Tissue sample from primary resection reveals highly cellular neoplasm exhibiting mitotically active nuclei (arrows) (H&E, X400). (B) Secondary resection was performed 10 mo after ^{131}I -81C6 monoclonal antibody treatment. Immunohistochemical stain for HAM56 (macrophage-related) marker indicates that the vast majority of cells in this infiltrate are macrophages (HAM56, X400).

after the patient's second higher radiation dose treatment, macrophages were present. This effect appears to be radiation related. For interstitial therapy, Fike et al. (18), by implanting nonradioactive brachytherapy seeds, noted that radiation therapy was required to increase the number of polymorphonuclear cells and that the inflammatory response was not simply related to the insult of seed placement. In addition, the rim is not simply the result of surgical insult. After temporal lobectomy for treatment of seizure disorder, no increase in FDG accumulation was noted at the surgical site (19). Thus, surgery and seed placement alone do not result in FDG accumulation on the PET scan.

A proposed mechanism for delayed immune response to radiation is the alteration of proteins by radiation, which then produce an allergic reaction (20). Radiation can prime microglial cells and astrocytes for tumor necrosis factor (TNF)-alpha production (21). Because heavy macrophage infiltration of radiation-damaged brain tissue is associated with areas of TNF-alpha and interleukin-6 expression, Kureshi et al. (20) suggest that TNF-alpha may mediate some delayed radiation-induced changes.

CONCLUSION

This study indicates that a metabolic rim of FDG accumulation may occur after ^{131}I -81C6 therapy in tumor cavities. The presence of a rim may be dose-dependent and is independent of the presence of malignant disease. Furthermore, the presence of nodularity is indicative of tumor recurrence.

REFERENCES

- Mahaley MS. Neurooncology index and review (adult primary brain tumors). Radiotherapy, chemotherapy, immunotherapy, photodynamic therapy. *J Neurooncol* 1991; 11:85-147.
- Baglan RJ, Marks JE. Soft-tissue reactions following irradiation of primary brain and pituitary tumors. *Int J Radiat Oncol Biol Phys* 1981;7:455-459.
- Marks JE, Wong J. The risk of cerebral radionecrosis in relation to dose, time and fractionation. *Prog Exp Tumor Res* 1985;29:210-218.
- Coffey RJ, Lunsford LD, Flickinger JC. The role of radiosurgery in the treatment of malignant brain tumors. *Neurosurg Clin North Am* 1992;3:231-244.
- Malkin MG. Interstitial brachytherapy of malignant gliomas: The Memorial Sloan-Kettering Cancer Center experience. *Recent Results Cancer Res* 1994;135:117-125.
- Loeffler JS, Alexander E, Wen Y, et al. Results of stereotactic brachytherapy used in the initial management of patients with glioblastoma. *J Natl Cancer Inst* 1990;24: 1918-1921.
- Loeffler JS, Alexander E, Shea WM, et al. Radiosurgery as part of the initial management of patients with malignant gliomas. *J Clin Oncol* 1991;10:1379-1385.
- Schold SC, Zalutsky MR, Coleman RE, et al. Distribution and dosimetry of I-123 labeled monoclonal antibody 81C6 in patients with anaplastic glioma. *Invest Radiol* 1993;29:488-496.
- Brown M, Coleman RE, Friedman A, et al. Intrathecal 131-I labeled antitenascin monoclonal antibody 81C6 treatment of patients with leptomeningeal neoplasms or primary brain tumor resection cavities with subarachnoid communication: phase I trial results. *Clin Cancer Res* 1996;2:963-972.
- Valk PE, Dillon WP. Radiation injury of the brain. *Am J Neuroradiol* 1991;12:45-62.
- Zalutsky MR, Moseley RP, Coakham HB, Coleman RE, Bigner DD. Pharmacokinetics and tumor localization of 131-I-labeled anti-tenascin monoclonal antibody 81C6 in patients with gliomas and other intracranial malignancies. *Cancer Res* 1989;49:2807-2813.
- Degrado TR, Turkington TG, Williams JJ, Stearns CW, Hoffman JM, Coleman RE. Performance characteristics of a whole-body PET scanner. *J Nucl Med* 1994;35:1398-1406.
- Akabani G, Poston JW, Bolch WE. Estimates of beta absorbed fractions in small tissue volumes for selected radionuclides. *J Nucl Med* 1991;32:835-839.
- Rozenal JM, Levine RL, Mahta MP, et al. Early changes in tumor metabolism after treatment: the effects of stereotactic radiotherapy. *Int J Radiat Oncol Biol Phys* 1991;20:1053-1060.
- Moringlane JR, Voges M, Huber G, Muller J, Leetz HK. Short-term CT and MR changes in brain tumors following ^{125}I interstitial irradiation. *J Comput Assist Tomogr* 1997;21:15-21.
- Halligan JB, Stelzer KJ, Rostomily RC, Spence AM, Griffin TW, Berger MS. Operation and permanent low-activity ^{125}I brachytherapy for recurrent high-grade astrocytomas. *Int J Radiat Oncol Biol Phys* 1996;35:541-547.
- Warnke PC, Hans FJ, Ostertag CB. Impact of stereotactic interstitial radiation on brain capillary physiology. *Acta Neurochir* 1993;58(suppl):85-88.
- Fike JR, Gobbel GT, Chou D, Wijnhoven B, Bellinzona M, Nakagawa M, Seilhan TM. Cellular proliferation and infiltration following interstitial irradiation of normal dog brain is altered by an inhibitor of polyamine synthesis. *Int J Radiat Oncol Biol Phys* 1995;32:1035-1045.
- Glantz MJ, Hoffman JM, Coleman RE, et al. Identification of early recurrence of primary central nervous system tumors by [^{18}F] fluorodeoxyglucose positron emission tomography. *Ann Neurol* 1991;29:347-355.
- Kureshi SA, Hoffman FM, Schneider JH, Chin LS, Apuzzo MLJ, Hinton DR. Cytokine expression in radiation-induced delayed cerebral injury. *Neurosurgery* 1994;35:822-830.
- Chiang CS, McBride WH. Radiation enhances tumor necrosis factor α production by murine brain cells. *Brain Res* 1991;566:265-269.